Journal of Magnetic Resonance 212 (2011) 249–253

Contents lists available at ScienceDirect

Journal of Magnetic Resonance

journal homepage: www.elsevier.com/locate/jmr

Using heat to control the sample spinning speed in MAS NMR

Eugene Mihaliuk, Terry Gullion *

Department of Chemistry, West Virginia University, Morgantown, WV 26506, United States

ARTICLE INFO

Article history:
Received 27 May 2011
Revised 11 July 2011
Available online 23 July 2011

Keywords:
Magic-angle spinning
Spinning speed
NMR
Heater
Air temperature

ABSTRACT

A new approach using temperature to control the spinning speed of a sample rotor in magic-angle spinning NMR is presented. Instead of an electro-mechanical valve that regulates the flow of drive gas to control the spinning speed in traditional MAS NMR systems, we use a small heater wire located directly in the stator. The sample spinning speed is controlled very accurately with a surprisingly low heating power of 1 W. Results on a benchtop unit demonstrate the capability of the system.

1. Introduction

Magic-angle sample spinning NMR (MAS NMR) has been used for over 50 years [1,2], with its popularity soaring after MAS was combined with cross-polarization [3–5] to provide high-resolution ^{13}C NMR spectra of macromolecules [6,7]. MAS NMR includes many experiments with rotor-synchronized radio-frequency pulse trains that necessitate controlling the spinning speed of the sample rotor to a set value [8,9]. For example, if the spinning speed of a ^{13}C-observe REAPDOR experiment is not controlled to within a few tenths of a Hz then the ^{13}C signal intensity arising from a site with a large chemical shift anisotropy is greatly reduced. Reduction in signal intensity is caused by the incomplete refocusing of the chemical shift anisotropy, which is caused by the REAPDOR pulse sequence being out of synchrony with the sample rotation when the spinning speed drifts from its set value. Sample spinning speeds are typically controlled using an optical detection system and feedback circuit that changes the flow of the drive gas through adjustments of a mechanical valve [10]. We describe a novel approach that uses heating of the drive gas to control the spinning speed.

Figs. 1 and 2 are presented first to show that heating the drive gas can control the spinning speed with remarkable precision. Fig. 1 shows the spinning speed (bottom) over a period of time starting with the controller off, followed by the controller on, and ending with the controller off. Noticeable fluctuations of the spinning speed are observed during the first 40 s shown in the figure where there is no active control. The nominal spinning speed is 5007 Hz with fluctuations of approximately +/− 1 Hz. When the controller is turned on during the next 160 s the spinning speed quickly moves to the set value of 5000 Hz. Very small fluctuations in the spinning speed are observed during active control. After the controller is inactivated, the spinning speed goes to approximately 5010 Hz with noticeable fluctuations. The applied heat is also shown in Fig. 1 (top) for reference. The heating power is set to a constant 1.3 W when control is off and is actively varied when the control is on. Fig. 2 shows two histograms of the spinning speed distributions for the situations when the controller is initially off (right) and when the controller is on (left). The bin size in the figure is 0.1 Hz, and each reported spinning speed was obtained by averaging over a 50 rotor-cycle time period. In the absence of control, there is a sizable distribution of spinning speeds with a mean value of 5007 Hz. The controlled experiment, however, is described by a very narrow distribution in spinning speeds. Approximately 80% and 98% of the recorded spinning speeds are within 0.1 Hz and 0.2 Hz, respectively, of the 5000 Hz set value. Tight control of the spinning speed was obtained solely by using heat to adjust the temperature of the drive gas.

2. Experimental

A modified Varian pencil rotor sample spinning [11,12] assembly with a 5 mm diameter rotor was used in this work. All experiments were performed on the bench and not as part of an NMR probe.

A Hydrovane rotary vane compressor (model HV07) operating at a nominal pressure of 105 psi is the source of the drive and bearing gas. The compressed air is initially delivered to a 100 gallon storage tank and then passed through a Zeks Hydronix two-stage

* Corresponding author. Fax: +1 304 293 4904.
E-mail address: terry.gullion@mail.wvu.edu (T. Gullion).

1090-7807/$ - see front matter © 2011 Elsevier Inc. All rights reserved.
doi:10.1016/j.jmr.2011.07.009

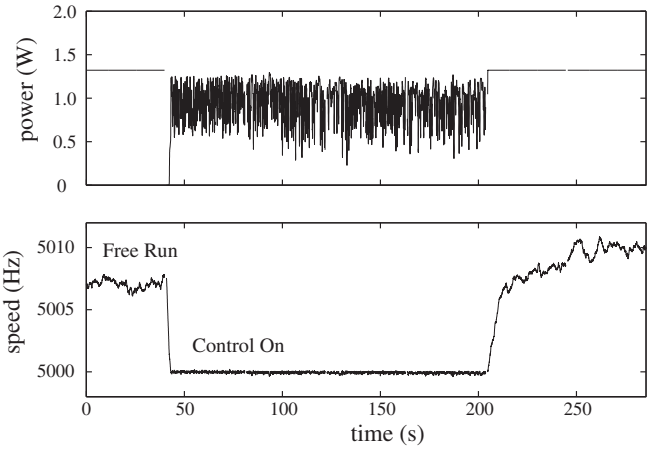

Fig. 1. Sample spinning speed with and without control. Measured spinning speeds (bottom) during times without active control are shown on the left and far right parts of the plot and show noticeable fluctuations. When the controller is on, the spinning speed is much more stable. The heating power during the time of the experiment is shown at the top.

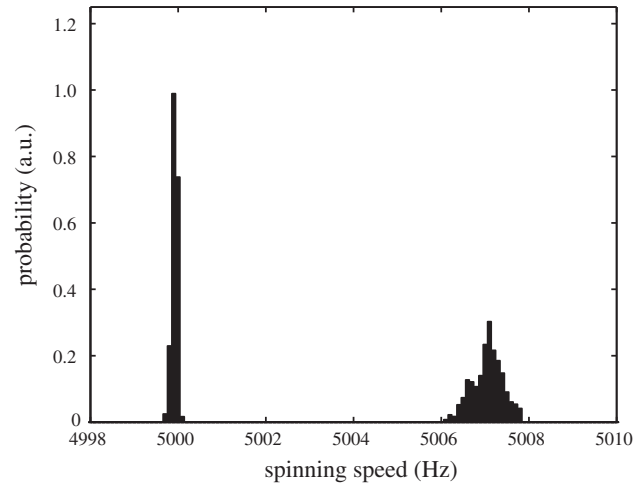

Fig. 2. Histograms of spinning speeds. The histogram on the right is spinning speeds without active control. The histogram on the left represents spinning speeds with the controller set to 5000 Hz.

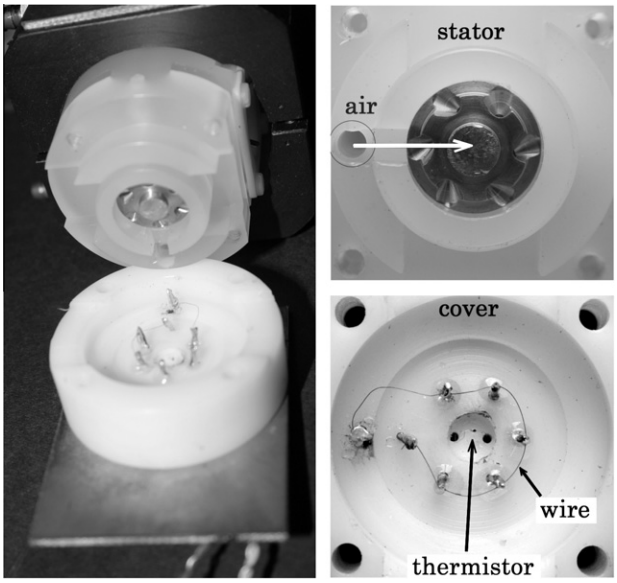

Fig. 3. Photograph of stator, brass nozzle piece, thermistor and wire. The diameter of the brass nozzle piece is 0.5 in. and serves as a size reference. The stator is made of Kel-F and the back plate housing the wire and thermistor is made of delrin.

desiccant dryer. These components are located in the attic four floors above our laboratory. A 1.25 in. diameter copper pipe brings the compressed air into our laboratory to feed a collection of storage tanks. In the laboratory, the compressed gas first enters a 60 gallon tank regulated at 90 psi and then enters a second 60 gallon tank regulated at 80 psi. Two lines come off the second 60 gallon tank. One line feeds a 30 gallon tank regulated at 40 psi and serves as the source of drive gas. The second line feeds another 30 gallon tank regulated at 50 psi and serves as the source of bearing gas. Particulate and oil filters are placed throughout the collection of air tanks. Manually adjustable regulators are used to set the pressure of the drive air and bearing air of the sample spinning assembly.

The base of the Varian spinning module, where the drive gas enters the stator and is forced through brass nozzles onto the rotor turbine, was modified to house a heater and a thermistor. Fig. 3 is a photograph showing the brass nozzle piece, stator, wire and thermistor. Fig. 4 is a drawing of the modified base plate of the stator with dimensions for reference. The heater was made from a loop of a single filament NbTi wire. This particular material has suitable resistivity and is non-magnetic. The filament was obtained by dissolving a 1 mm diameter copper matrix superconductive magnet wire in 1 M nitric acid overnight. Prior to the acid treatment, the outer insulation was removed with fine sandpaper. The diameter of the heater wire is approximately two thousandths of an inch. The length of the wire is 1.7 in. and its room-temperature resistance is 11.4 ohm; the resistivity increases slightly at full power. A voltage of 0–6 V applied to the wire generates 0–3.0 W of power for heating the drive gas. The flow rate of the drive gas is approximately 1 standard L/s. The combination of high air velocity and small wire diameter produces a very fast (millisecond time scale) response in drive air temperature to the supplied electrical power. The drive gas temperature is also moderated by contact with the thermal reservoirs associated with the brass nozzle and surrounding stator components. The temperature is measured before the gas enters the drive nozzles with a 0.013 in. diameter micro-bead thermistor (Veeco 42A29).

The spinning speed is measured using an optical detection system. The sample rotor is etched with a single black mark and is illuminated with a laser diode operating at 30 mW and 635 nm. The reflected light is captured by a lens to create a $\times 10$ magnified image of the rotor which is focused onto a 0.2 mm slit just in front of a photodiode (EG&G Photon Devices DT-25). The photodiode converts the detected light into an analog electrical signal. The photodiode current is amplified in two steps by operational amplifiers (Analog Devices OP-37) and shaped into logic pulses by a Schmitt trigger inverter (74HC14), with the edges of the pulses representing the transitions between the light colored rotor wall and the dark engraved etching on the rotor. Fiber optic tachometers in most MAS NMR probes exhibit random jitter in the output pulse timing on the order of multiple microseconds with respect to the true rotational position of the rotor. This jitter is the dominant limiting factor in rapid measurement of spinning speed. The purpose of our focusing lens and slit is to reduce the jitter to 0.3 μs to allow a more rapid and more accurate measurement of the spinning speed.

The controller determines the spinning speed by measuring the duration of rotor periods. The tachometer pulses are fed into a microcontroller (Microchip dsPIC30F2010), and an edge capture unit in the microcontroller determines the time of the falling edge

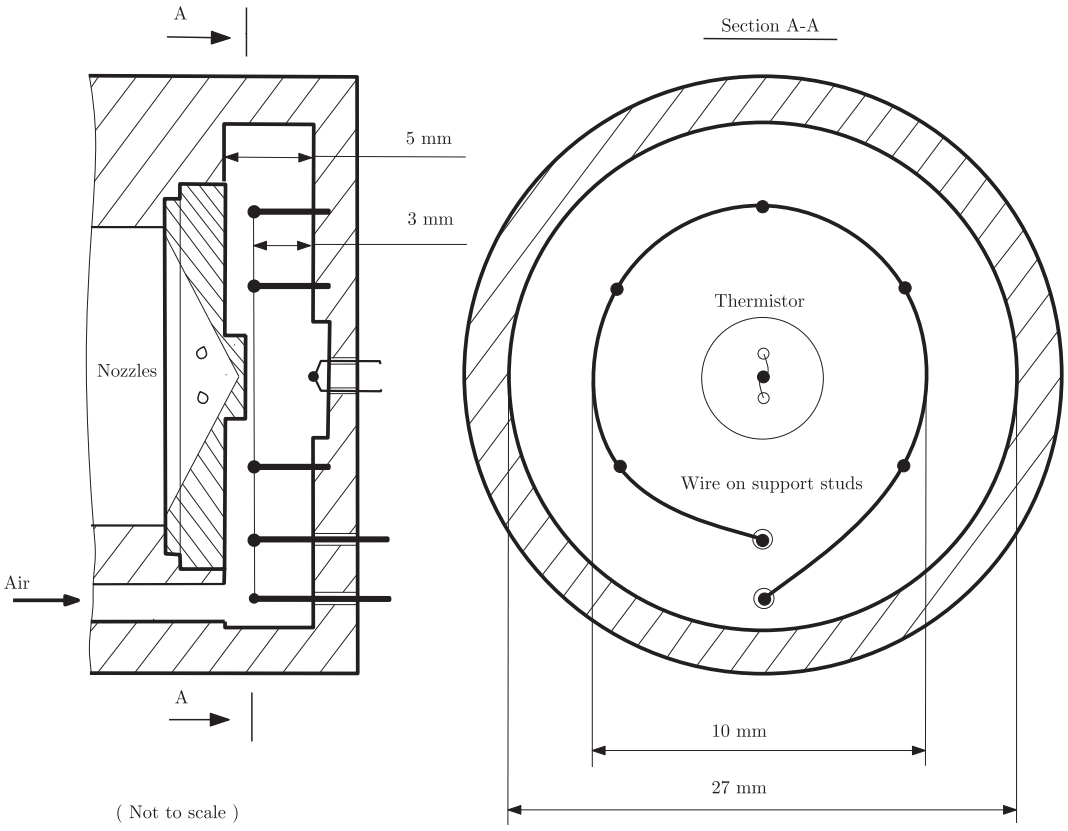

Fig. 4. Drawing of the modified base plate of the stator.

of each pulse. The microcontroller clock frequency is 20 MHz, which gives 50 ns time resolution. However, the approximately 0.3 μs of jitter still present in our optical pickup system dominates the uncertainty of the time measurement and determines the accuracy to which the spinning speed can be determined. Measuring individual rotor periods provides the most up-to-date spinning speed data, but the signal is noisy ($\sigma = \frac{0.3\ \mu s}{200\ \mu s} \times 5000\ \text{Hz} = 7.5\ \text{Hz}$). Measuring over N rotor periods reduces the noise to 1/N, but the data rate becomes proportionally slower. In practice, the controller uses an exponential moving average method. After successive rotor periods, τ_i, are measured individually, the resulting values are filtered by a simple low-pass filter with an exponential decay impulse response. This type of averaging weights the most recent rotor cycles more heavily than past rotor cycles while still providing a benefit of averaging over time, which is determined by the decay rate of the filter. The average rotor period, $\bar{\tau}_i$, is calculated as $\bar{\tau}_i = (1-\eta)\bar{\tau}_{i-1} + \eta\tau_i$. The weighting factor, η, is set to 1/16 for the results presented here. Although this may not appear to sufficiently remove jitter-induced spinning speed variance, the control involves several other components with relatively long time constants (such as rotor inertia) which effectively provide further averaging. The difference between the measured average spinning speed and the set spinning speed serves as the input to a proportional-integral-derivative (PID) controller. The output of the controller is a DC voltage between 0 and 6 V that is applied to the NbTi wire to produce 0–3.0 W of heating power. The voltage applied to the heater is updated every rotor cycle. In normal operation, the baseline heater power is set to 1.3 W and the drive air input is manually adjusted with a pressure regulator to approximate the desired set frequency before the controller is activated. Additional heating power will increase the spinning speed and reduced power will lower the spinning speed.

3. Results

Fig. 5 shows the temperature of the drive air as a function of heater power. This power is applied continuously during measurements. The drive air temperature has a linear dependence on heater power over this range of power and increases by 3.5 °C when full power is applied. However, the sample temperature would not rise by this amount because the bearing air is not heated and

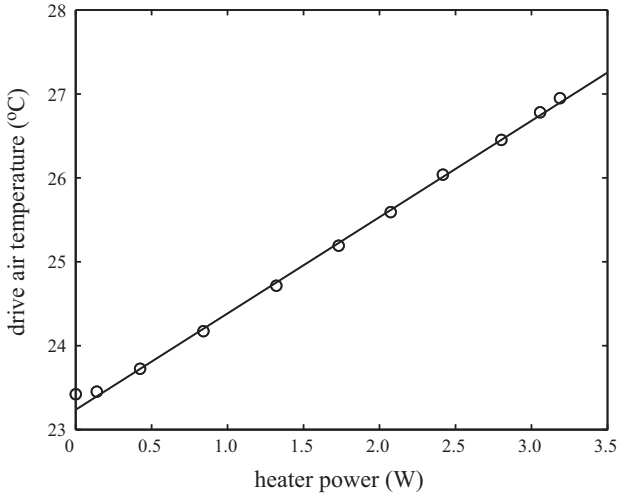

Fig. 5. Drive air temperature versus heater power. The drive air temperature measured just before the air enters the nozzles shows a linear dependence on heater power with a dependence of approximately 1.2 °C/W for the conditions described for this work.

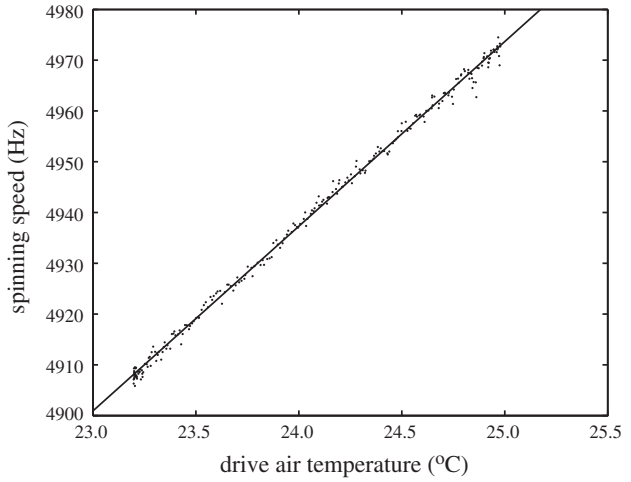

Fig. 6. Spinning speed dependence on drive gas temperature. The spinning speed shows a linear dependence on drive air temperature given by approximately 18 Hz/°C.

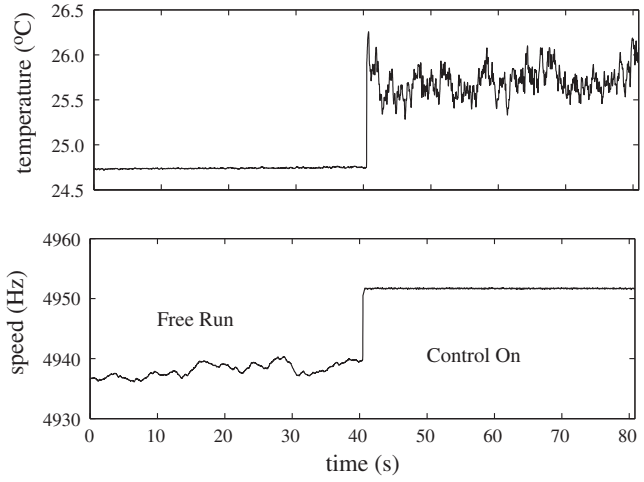

Fig. 7. Influence of the temperature of the drive gas on spinning speed. The bottom plot shows the spinning speed without control (first 40 s) and with control (after 40 s). The top plot shows the corresponding temperature of the drive gas. The temperature is constant in the absence of control because 1.3 W of heating is applied constantly. The temperature of the drive gas changes when active control is applied because the heater is working to stabilize the spinning speed.

would serve to keep the sample from heating. The temperature rise of the drive gas is a modest 1 °C at 1 W continuous heating.

Fig. 6 shows a dependence of spinning speed on drive air temperature (measured on the heater side of the nozzle) of 18 Hz/°C. Clearly, small changes in drive gas temperature can affect the spinning speed. Fig. 7 shows the spinning speed (bottom) during time intervals without active control and with active control. In the absence of active control the heater is set to 1.3 W and the drive temperature is 24.7 °C. During this time the spinning speed fluctuates by about 2 Hz for this data set. When control is applied the spinning speed goes to the set value of 4952 Hz with very little fluctuations. The drive air temperature (top) during the control period has a nominal value of 25.7 °C and changes by approximately ±0.3 °C as the heater power circuit works to maintain the spinning speed. Sample temperatures would not be significantly altered using this heating system to control the spinning speed.

The histogram of the controlled spinning speed presented in Fig. 2 illustrates that the spinning speed is tightly controlled. Over 98% of measured rotor speeds are within 0.2 Hz of the set value and most of these are within 0.1 Hz of the set value. Spinning speeds are determined by averaging over 50 rotor cycles; thus, the histogram shows the spinning speeds present during the time scales of an NMR pulse sequence. A set spinning speed of 5000 Hz has a rotor period of 200 μs, and if the spinning speed differs by 0.2 Hz from this set value, then the average rotor period differs by approximately 0.008 μs from 200 μs. For rotor synchronous rf pulse trains, this small time differential should have minimal effects on NMR experiments. For example, a 100 rotor cycle evolution period in an NMR experiment is timed for 20 ms with a set spinning speed of 5000 Hz. If the experiment occurs while the spinning speed is at 5000.2 Hz, the pulse train ends 0.8 μs after the 100th rotor cycle is completed. Thus, at the end of the 100 rotor cycle experiment the rotor is out of phase from the ideal position by only 1.4°.

4. Conclusions

Temperature of the drive gas has a considerable effect on the spinning speed of a MAS rotor. The spinning speed dependence on drive gas temperature is approximately 1 Hz per 0.05 °C for our system. This indicates the potential importance of this often-neglected parameter in MAS NMR either as a way to control the spinning speed (as shown here) or possibly as a concern for possible drifts in spinning speed caused by temperature changes. Active control of the drive gas temperature in a pencil style rotor system can be used to control the spinning speed. With the heater at the base of the rotor assembly and with appropriate design of the control system, corrections to the spinning speed can occur quickly. The sample spinning speed distribution is quite narrow and should be useful for rotor synchronized pulse sequences, especially those designed to take advantage of large interactions evolving during the NMR experiment. Although the results presented here were obtained on a benchtop assembly, it should be relatively straightforward and inexpensive to implement the system into MAS NMR probes and such efforts are underway.

Constant mass flow provides a qualitative description of how the system works. The drive gas set-up for the experiments described in this paper is best described as a constant flow system. Hence, the mass flow into and out of the heating chamber is constant, and is not significantly dependent on the temperature of the heater. The action of increasing the drive gas temperature is to lower the density of the gas while increasing the volume per unit mass of gas. As a consequence, the increased volume of unit mass of gas must exit the drive nozzles at a higher velocity thereby increasing the spinning speed of the rotor.

Acknowledgment

This work was supported by Grant CHE-0846583 from the National Science Foundation.

References

[1] I.J. Lowe, Free induction decays of rotating solids, Phys. Rev. Lett. 2 (1959) 285–287.
[2] E.R. Andrew, A. Bradbury, R.G. Eades, Removal of dipolar broadening of nuclear magnetic resonance spectra of solids by speciman rotation, Nature 183 (1959) 1802–1803.
[3] S.R. Hartmann, E.L. Hahn, Nuclear double resonance in the rotating frame, Phys. Rev. 128 (1962) 2042–2053.
[4] A. Pines, M.G. Gibby, J.S. Waugh, Proton-enhanced nuclear induction spectroscopy, J. Chem. Phys. 56 (1971) 1776–1777.
[5] A. Pines, M.G. Gibby, J.S. Waugh, Proton-enhanced NMR of dilute spins in solids 59 (1973) 569–590.
[6] J. Schaefer, E.O. Stejskal, Carbon-13 nuclear magnetic resonance of polymers spinning at the magic angle, J. Am. Chem. Soc. 98 (1976) 1031–1032.
[7] E.O. Stejskal, J. Schaefer, J.S. Waugh, Magic-angle spinning and polarization transfer in proton-enhanced NMR, J. Magn. Reson. 28 (1977) 105–112.

[8] K. Schmidt-Rohr, H.W. Spiess, Multidimensional Solid-State NMR and Polymers, Academic Press, San Diego, 1994.
[9] M.J. Duer, Solid-State NMR Spectroscopy Principles and Applications, Blackwell Science, Oxford, 2002.
[10] J.N. Lee, D.W. Alderman, J.Y. Jin, K.W. Zilm, C.L. Mayne, R.J. Pugmire, D.M. Grant, Cylindrical spinner and speed controller for magic angle spinning nuclear magnetic resonance, Rev. Sci. Instrum. 55 (1984) 516–520.
[11] V.J. Bartuska, D.H. Lewis, R.B. Lewis, D.G. Dalbow, US Patent 4511841.
[12] F.D. Doty, Solid state NMR probe design, in: D.M. Grant, R.K. Harris (Eds.), Encyclopedia of Nuclear Magnetic Resonance, vol. 7, Chichester, 1996, pp. 4475–4485.